

Modeling for Control of HCCI Engines

Gregory M. Shaver

J.Christian Gerdes

Parag Jain

Design Division
Dept. of Mechanical Engineering
Stanford University
Stanford, California 94305-4021
Email: shaver@stanford.edu

Design Division
Dept. of Mechanical Engineering
Stanford University
Stanford, California 94305-4021
Email: gerdes@cdr.stanford.edu

Design Division
Dept. of Mechanical Engineering
Stanford University
Stanford, California 94305-4021
Email: paragjain@freightliner.com

P.A. Caton

C.F. Edwards

Thermosciences Division
Dept. of Mechanical Engineering
Stanford University
Stanford, California 94305-4021
Email: patcaton@stanford.edu

Thermosciences Division
Dept. of Mechanical Engineering
Stanford University
Stanford, California 94305-4021
Email: edwards@navier.stanford.edu

Abstract

The goal of this work is to accurately predict the phasing of HCCI combustion for a single cylinder research engine using variable valve actuation (VVA) at Stanford University. Three simple single-zone models were developed and compared with experiment. The difference between the three modeling approaches centered around the combustion chemistry mechanism used in each. The first modeling approach, which utilized a temperature threshold to model the onset of the combustion reaction, did not work well. However, an integrated reaction rate threshold accounting for both the temperature and concentration did correlate well with experiment. Additionally, another model utilizing a simple two-step kinetic mechanism also showed good correlation with experimental combustion phasing.

1 Introduction

Experimental studies at Stanford University ([1], [4]) and elsewhere [6] demonstrate that variable valve actuation (VVA) can be used to initiate homogeneous charge compression ignition (HCCI). This is achieved by reinducting combustion products from the previous cycle, thereby increasing the sensible energy of the reactant charge and allowing ignition to occur by compression alone at modest compression ratios. Since the reinducted products act as a thermal sink during combustion, this process lowers the peak combustion temperature, which in turn lowers NO_x concentrations. This drop in NO_x is one of the major bene-

fits of HCCI. It is important to note that other methods exist to initiate HCCI, such as heating or precompressing the intake air ([10],[7]) or varying the compression ratio [2].

Due to the nature of HCCI, a fundamental control challenge exists. Unlike spark ignition (SI) or diesel engines, where the combustion is initiated via spark and fuel injection, respectively, HCCI has no specific event that initiates combustion. Therefore, ensuring that combustion occurs with acceptable timing is more complicated than in the case of either SI or diesel combustion. HCCI combustion timing is dominated by chemical kinetics, which depends on in-cylinder species concentrations, temperature and pressure. These parameters are controlled in the system studied through the use of the fully flexible VVA system.

To synthesize a controller to stabilize HCCI using the VVA system, a model of the system with special attention paid to combustion phasing is therefore necessary. This model should be as simple as possible, as it is often difficult to synthesize controllers from more complex models. This paper describes three fairly simple models and compares them to behavior seen on a single-cylinder research engine outfitted with a fully flexible VVA system. Each model tracks the in-cylinder pressure, temperature and species concentrations during an HCCI cycle. The complete cycle includes the concurrent induction of the reactants through the intake valve and the products of combustion from the previous cycle through the exhaust valve, compression, expansion and exhaust. The valve flow during the induction and exhaust portions of the cycle are modeled with compressible, steady state, one-dimensional, isentropic flow relations. The three

models differ only in the approach used to model the combustion chemistry. In the first model, the simplest of the three, a temperature threshold is used to model the onset of combustion. This approach shows poor correlation with experiment, failing to capture the dependence of combustion timing on concentration. In the second model, a two step mechanism implementing a series of Arrhenius reaction rates is used. Good correlation with experiment with respect to phasing is found, with slight discrepancy in pressure at the initiation of combustion. The third model implements elements from the other two models through the use of an integrated Arrhenius rate as a threshold value. This approach shows good correlation with experiment, but shows slight discrepancy as combustion completes.

Various types of models of HCCI combustion with more complexity than those presented here have been developed. These include multi-zone models ([8], [3]) and multi-dimensional CFD models [5]. While these approaches can be expected to more accurately predict the performance and emissions in HCCI combustion, the goal of this work is to develop simple models characterizing combustion phasing. It is from the simplified models that controllers may more readily be synthesized to stabilize the HCCI combustion during load tracking.

2 Modeling Approach

For each of the three approaches investigated, the modeling was based on an open system first law analysis, with steady state compressible flow relations used to model the mass flow through the intake and exhaust valves. The model includes nine states: the temperature, T ; the concentrations of propane, $[C_3H_8]$, oxygen, $[O_2]$, Nitrogen, $[N_2]$, carbon dioxide, $[CO_2]$, water, $[H_2O]$, and carbon monoxide, $[CO]$; the crank angle, θ ; and the cylinder volume, V .

2.1 Volume Rate Equation

The in-cylinder volume and its derivative are given by the following well-known slider-crank formulas:

$$V = V_c + \frac{\pi B^2}{4} (l - a - a \cos \theta - \sqrt{l^2 - a^2 \sin^2 \theta}) \quad (1)$$

$$\dot{V} = \frac{\pi}{4} B^2 a \dot{\theta} \sin \theta \left(1 + a \frac{\cos \theta}{\sqrt{l^2 - a^2 \sin^2 \theta}} \right) \quad (2)$$

with:

$$\dot{\theta} = \omega \quad (3)$$

where ω is the rotational speed of the crankshaft, a is half of the stroke length, L is the connecting rod length, B is the bore diameter and V_c is the clearance volume at top dead center.

2.2 Valve Flow Equations

The mass flow through the valves consists of flow from intake manifold to cylinder, \dot{m}_1 , from cylinder to exhaust

manifold, \dot{m}_2 , and from exhaust manifold to cylinder, \dot{m}_3 , as shown in Figure 1. Equations for these mass flow

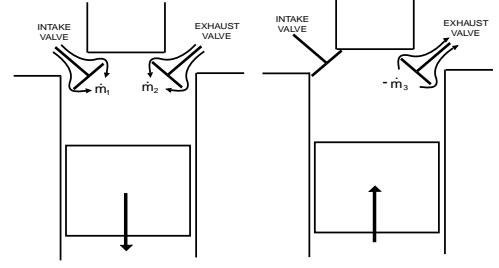


Figure 1: Valve Mass Flows: left - induction with intake and exhaust valves open, right - exhaust

rates are developed using a compressible, steady state, one-dimensional, isentropic flow analysis for a restriction, where real gas flow effects are included by means of a discharge coefficient, C_D . The relations for the mass flows are:

$$\dot{m} = \frac{C_D A_R p_o}{\sqrt{RT_o}} \left(\frac{p_T}{p_o} \right)^{1/\gamma} \left[\frac{2\gamma}{\gamma-1} \left[1 - \left(\frac{p_T}{p_o} \right)^{(\gamma-1)/\gamma} \right] \right] \quad (4)$$

for unchoked flow ($p_T/p_o > [2/(\gamma+1)]^{\gamma/(\gamma-1)}$), and:

$$\dot{m} = \frac{C_D A_R p_o}{\sqrt{RT_o}} \sqrt{\gamma} \left[\frac{2}{\gamma+1} \right]^{(\gamma+1)/2(\gamma-1)} \quad (5)$$

for choked flow ($p_T/p_o \leq [2/(\gamma+1)]^{\gamma/(\gamma-1)}$), where A_R is the effective open area for the valve, p_o is the upstream stagnation pressure, T_o is the downstream stagnation temperature and p_T is the downstream stagnation pressure.

Figure 2 shows the general shape of a valve area profile used for comparison between model and experiment. It is the intake valve opening (IVO) and exhaust valve closing (EVC) locations that are varied for different operating conditions. For the mass flow of the reactant gas into the

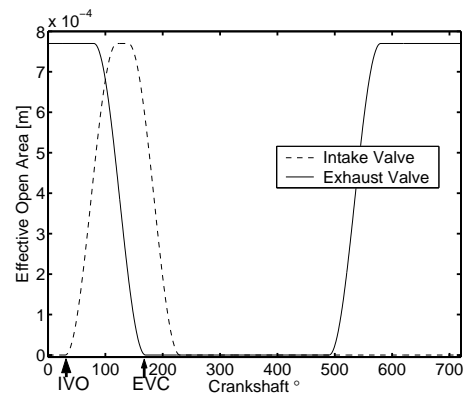


Figure 2: General Valve Profile

cylinder through the intake valve, \dot{m}_1 , p_o is the intake manifold pressure, assumed to be atmospheric, and p_T is the cylinder pressure, p . For the mass flow of burnt products

out of the cylinder through the exhaust valve, \dot{m}_2 , p_o is the cylinder pressure, p , and p_T is the exhaust manifold pressure, assumed to be atmospheric. For the reinducted exhaust from the previous cycle through the exhaust valve, \dot{m}_3 , p_o is the exhaust manifold pressure, and p_T is the cylinder pressure, p . Setting the manifold pressure to atmospheric is an approximation. Strategies to model manifold flow dynamics are available [9], and could be implemented here in a straightforward way to describe manifold pressure fluctuations. Note that it is assumed that there is no flow from cylinder to intake manifold. This is a reasonable assumption for the experimental system studied in this paper. However, allowing flow from cylinder to intake manifold is straightforward if desired.

2.3 Concentration Rate Equations

The rate of change of concentration for species i , $[\dot{X}_i]$ is related to number of moles of species i in the cylinder, N_i , by:

$$[\dot{X}_i] = \frac{d}{dt} \left(\frac{N_i}{V} \right) = \frac{\dot{N}_i}{V} - \frac{\dot{V}N_i}{V^2} = w_i - \frac{\dot{V}N_i}{V^2} \quad (6)$$

where w_i , the rate of change of moles of species i per unit volume has been defined as:

$$w_i = \frac{\dot{N}_i}{V} \quad (7)$$

It has two contributions: the rate of change of moles of species i per unit volume due to the combustion reactions, $w_{rxn,i}$, and due to flow through the valves under the control of the VVA system, $w_{valves,i}$, such that:

$$w_i = w_{rxn,i} + w_{valves,i} \quad (8)$$

The combustion reaction rate, $w_{rxn,i}$, is determined through the use of a combustion chemistry mechanism. As noted, the mechanism used is the difference between the three models presented in this paper. These approaches will be outlined in Section 3.

Given the mass flow rates (\dot{m}_1 , \dot{m}_2 and \dot{m}_3) from the analysis in Section 2.2, the rate of change of moles of species i per unit volume due to flow through the valves, $w_{valves,i}$, can be found using the species mass fractions:

$$w_{valves,i} = w_{1,i} + w_{2,i} + w_{3,i} \quad (9)$$

where:

$$w_{1,i} = \frac{Y_{1,i}\dot{m}_1}{VMW_i} \quad (10)$$

$$w_{2,i} = \frac{Y_{2,i}\dot{m}_2}{VMW_i} \quad (11)$$

$$w_{3,i} = \frac{Y_{3,i}\dot{m}_3}{VMW_i} \quad (12)$$

Here $Y_{1,i}$, $Y_{2,i}$ and $Y_{3,i}$ are the mass fractions of species i in the inlet manifold, exhaust manifold and cylinder, respectively. It is assumed that a stoichiometric mixture is present

in the intake manifold. Further, it is assumed that only the major combustion products of CO_2 , H_2O and N_2 are re-inducted into the cylinder through the exhaust. Therefore $Y_{1,i}$ and $Y_{2,i}$ are constant. Note that other intake and exhaust manifold compositions can be considered, but in any case the manifold mass fractions are constant during an engine cycle. However, the mass fraction of species i in the cylinder, $Y_{3,i}$, is constantly changing, and can be related to the concentration states as:

$$Y_{3,i} = \frac{[X_i]MW_i}{\sum [X_i]MW_i} \quad (13)$$

2.4 Temperature Rate Equations

In order to derive a differential equation for the temperature of the gas inside the cylinder, the first law of thermodynamics for an open system and the ideal gas law are combined as outlined below. The first law of thermodynamics for an open system is:

$$\frac{d(mu)}{dt} = Q - W + \dot{m}_1h_1 + \dot{m}_2h_2 + \dot{m}_3h_3 \quad (14)$$

where m is the mass of species in the cylinder, u is the internal energy, Q is the heat transfer rate, W is the work, h_1 is the enthalpy of species in the intake manifold, h_2 is the enthalpy of species in the exhaust manifold, and h_3 is the enthalpy of the species in the cylinder. For the case of the piston cylinder the work is:

$$W = p\dot{V} \quad (15)$$

where v is the specific volume of the gas in the cylinder. Now, given that the enthalpy is related to the internal energy as:

$$h = u + pv \quad (16)$$

Equations 14,15 and 16 can be combined to yield:

$$\frac{d(mh)}{dt} = \dot{m}pV/m + \dot{p}V + \dot{m}_1h_1 + \dot{m}_2h_2 + \dot{m}_3h_3 \quad (17)$$

Expansion of the enthalpy to show the contributions of the species in the cylinder can be represented as:

$$mh = H = \sum N_i\hat{h}_i \quad (18)$$

where N_i is the number of moles of species i in the cylinder, and H is the total enthalpy of species in Joules in the cylinder, and \hat{h}_i is the enthalpy of species i on a molar basis.

Noting that the rate of change of enthalpy per unit mole of species i can be represented as $\hat{h}_i = c_{p,i}(T)\dot{T}$, where $c_{p,i}(T)$ is the specific heat of species i per mole at temperature T , Equations 18 and 6 can be combined to give:

$$\frac{d(mh)}{dt} = V \left(\sum [\dot{X}_i]\hat{h}_i + \dot{T} \sum [X_i]c_{p,i}(T) \right) + \dot{V} \sum [X_i]\hat{h}_i \quad (19)$$

In-cylinder pressure and its derivative can be related to the concentrations and temperature through the ideal gas law as:

$$p = \sum [X_i]RT \quad (20)$$

$$\dot{p} = \frac{p \sum [\dot{X}_i]}{\sum [X_i]} + \frac{p \dot{T}}{T} \quad (21)$$

Meanwhile, the in cylinder mass and its derivative may be related to the species concentrations, molecular weights and volume as:

$$m = V \sum [X_i]MW_i \quad (22)$$

$$\dot{m} = \dot{V} \sum [X_i]MW_i + V \sum [\dot{X}_i]MW_i \quad (23)$$

Equating the right sides of Equations 17 and 19, substituting Equations 21, 22, and 23, and rearranging yields a differential equation for temperature:

$$\dot{T} = \frac{-(\sum [\dot{X}_i]\hat{h}_i) - \frac{\dot{V}(\sum [X_i]\hat{h}_i)}{V} + \frac{p \sum [\dot{X}_i]}{\sum [X_i]} + \frac{\sum \dot{m}_i \hat{h}_i}{V}}{(\sum [X_i]\hat{c}_{p,i}(T)) - p/T} \quad (24)$$

Equations 2, 3, 6 and 24 represent the set of nonlinear differential equations for each of the nine states used in each of the models. As noted, the combustion reaction rate, $w_{rxn,i}$, in Equation 6 is modeled differently in each of the approaches as outlined in the next section.

3 Combustion Chemistry Modeling

The combustion chemistry mechanism utilized is the difference between the three modeling approaches. For all three approaches, the stoichiometric reaction of propane and air is assumed since this is the case for the experimental data for which model results are compared. The major products assumption is also made, such that the global reaction for combustion can be written as:



3.1 Temperature Threshold Approach

As a first pass a simple temperature threshold method was developed in which the combustion reactions are assumed to start once the in-cylinder temperature reaches a critical value. In this case, the rate of reaction of the propane is approximated as being gaussian in nature, such that:

$$w_{C_3H_8} = \begin{cases} \frac{[C_3H_8]_i V_i \bar{\theta} \exp\left[\frac{-((\theta - \theta_{init}) - \bar{\theta})^2}{2\sigma^2}\right]}{V \sigma \sqrt{2\pi}} & T \geq T_{th} \\ 0 & T < T_{th} \end{cases} \quad (26)$$

where θ_{init} , V_i and $[C_3H_8]_i$ are the crank angle, volume and propane concentration, respectively, at the point where combustion begins (i.e. where $T = T_{th}$). Further, σ and $\bar{\theta}$ are the standard deviation and mean associated with the gaussian

reaction rate expression, and are fitted to correlate with experiment at one operating condition. Note that other functions could be used to model the reaction rate of propane, such as a Wiebe function.

By inspection of equation 25 the reaction rates of the other species follow directly:

$$w_{O_2} = 3.5w_{C_3H_8} \quad (27)$$

$$w_{N_2} = 0 \quad (28)$$

$$w_{CO_2} = -3w_{C_3H_8} \quad (29)$$

$$w_{H_2O} = -4w_{C_3H_8} \quad (30)$$

Figures 3 and 4 show that a single temperature threshold fails to capture combustion phasing at different operating conditions. This is due to the fact the initiation of the combustion reaction depends not only on the temperature, but also the concentration of species present in-cylinder. This dependence on both temperature and concentrations is especially important in the case of HCCI, where reinducted exhaust species from the previous cycle both dilute and heat the reactant species. While the dilution of reactants decreases the likelihood of combustion, the reactant heating increases the likelihood of combustion. The interplay of these two phenomena leads to a self-stabilizing effect, which corresponds to experimental observations of HCCI using VVA.

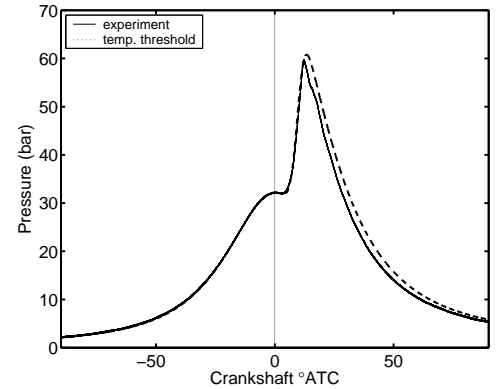
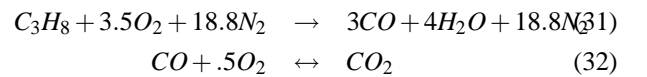


Figure 3: Temperature Threshold Approach: IVO @ 25deg., EVC @ 165

3.2 Two Step Mechanism

In order to capture the effects of both concentration and temperature on combustion timing, a more detailed, yet still simple, approach to modeling the combustion kinetics was developed. In this case the reaction rate expressions depend directly on both concentration and temperature using well-known Arrhenius-type relations. Consider the two-step mechanism:



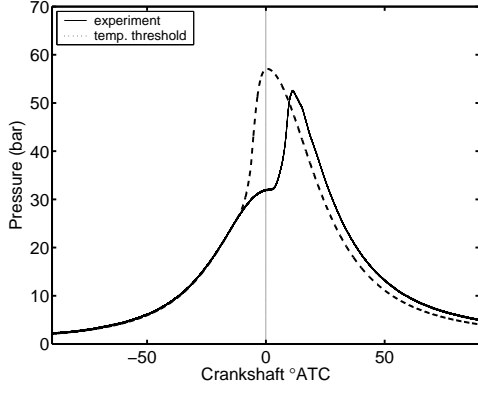


Figure 4: Temperature Threshold Approach: IVO @ 45deg., EVC @ 185

The reaction rates for C_3H_8 oxidation and CO oxidation are given in [11] as:

$$w_{C_3H_8} = 4.83e^9 \exp\left(\frac{-15098}{T}\right) [C_3H_8]^{-1} [O_2]^{1.65} \quad (33)$$

$$w_{CO,ox} = 2.24e^{12} \exp\left(\frac{-20130}{T}\right) [CO][H_2O]^{-5} [O_2]^{.25} - 5e^8 \exp\left(\frac{-20130}{T}\right) [CO_2] \quad (34)$$

These Arrhenius-type relations are commonly used to model reaction rates in combustion mechanisms. By inspection of equation 32, the other reaction rates follow as:

$$w_{O_2} = 3.5w_{C_3H_8} + .5w_{CO,ox} \quad (35)$$

$$w_{N_2} = 0 \quad (36)$$

$$w_{CO_2} = -w_{CO,ox} \quad (37)$$

$$w_{H_2O} = -4w_{C_3H_8} \quad (38)$$

$$w_{CO} = -3w_{C_3H_8} + w_{CO,ox} \quad (39)$$

Note that in this approach there is no need to track any threshold values. Results for this approach (Figures 5

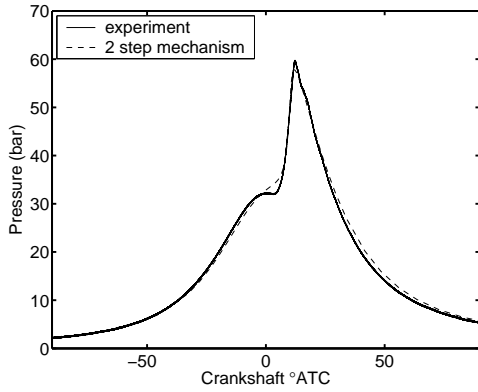


Figure 5: Two Step Mechanism Approach: IVO @ 25deg., EVC @ 165

and 6) show good correlation with experiment with respect to combustion phasing, pressure rise, pressure decay and peak pressure. However, there is a discrepancy in pressure around the onset of combustion. More detailed mechanisms, with more reactions and corresponding Arrhenius

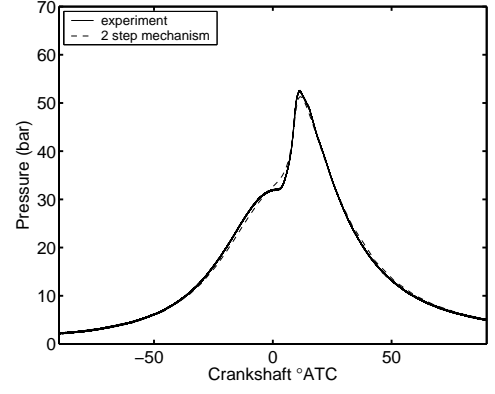


Figure 6: Two Step Mechanism Approach: IVO @ 45deg., EVC @ 185

reaction rate expressions can be implemented in a comparable way as the simple two step mechanism and be expected to show better correlation with experiment. However, the goal here is to keep the overall model simple, while still capturing the combustion phasing and overall behavior. The two step approach accomplishes this fairly well. It is also clear through comparison with the temperature threshold approach that both concentration and temperature must be considered when modeling combustion timing.

3.3 Integrated Global Arrhenius Rate Threshold

The conclusion that both temperature and concentration should be included in a description of combustion initiation motivated a new approach with elements from both of the previous approaches. In this case the proposed rate of reaction of the propane is the same as that used for the temperature threshold approach. Additionally, the idea of a threshold parameter to mark the onset of combustion was also adopted from the temperature threshold approach. The difference is that the threshold used is the integration of an Arrhenius type reaction rate expression similar to those used in the two step mechanism approach, instead of a temperature. This integrated reaction rate, $\int RR$, then takes the form:

$$\int RR = \int_0^\theta AT^n \exp(E_a/(RT)) [C_3H_8]^a [O_2]^b d\theta \quad (40)$$

such that:

$$w_{C_3H_8} = \begin{cases} \frac{[C_3H_8]_i V_i \theta \exp\left[\frac{-((\theta - \theta_{init}) - \bar{\theta})}{2\sigma^2}\right]}{V\sigma\sqrt{2\pi}} & \int RR \geq \int RR_{th} \\ 0 & \int RR < \int RR_{th} \end{cases} \quad (41)$$

where the threshold value of the integrated reaction rate, $\int RR_{th}$, has a value which correlates experiment and model at one operating condition. By inspection of equation 25 the reaction rates of the other species can be deduced as:

$$w_{O_2} = 3.5w_{C_3H_8} \quad (42)$$

$$w_{N_2} = 0 \quad (43)$$

$$w_{CO_2} = -3w_{C_3H_8} \quad (44)$$

$$w_{H_2O} = -4w_{C_3H_8} \quad (45)$$

Like the results for the two step model, the predicted com-

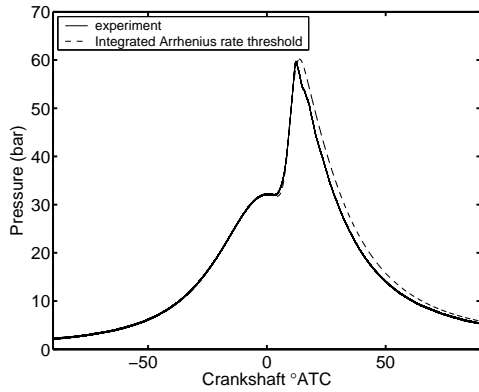


Figure 7: Integrated Arrhenius Rate Threshold Approach: IVO @ 25deg., EVC @ 165

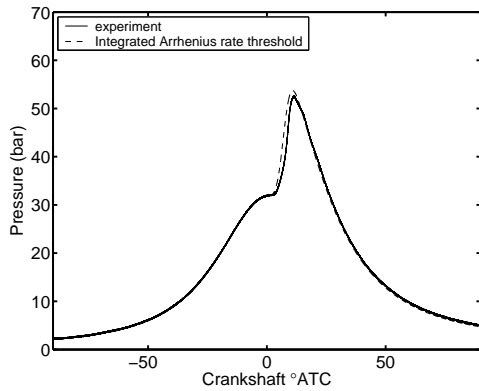


Figure 8: Integrated Arrhenius Rate Threshold Approach: IVO @ 45deg., EVC @ 185

bustion phasing with the integrated rate threshold approach correlated with experiment, as can be seen in Figures 7 and 8. Furthermore, the pressure near the onset of combustion matched experiment much better than the two step model. However, slight discrepancies in pressure rise, maximum pressure and pressure decrease can be noted along the pressure peak.

4 Conclusion

Three different modeling strategies were developed and compared to experimental results. The main difference among the three approaches was how the chemical kinetics were modeled. In the simplest approach the kinetics were assumed initiated once a temperature threshold was attained. Following the crossing of this threshold, the rate of consumption of mass of propane was approximated as

a gaussian like function. This approach showed unsatisfactory results with significant deviations from experiment. These deviations were attributed to the fact that species concentrations were not used to describe the combustion initiation threshold. The second approach implemented a simple two step mechanism, with Arrhenius-type reaction rates for the oxidation of propane and carbon monoxide. Although this method predicted combustion phasing well, it was desirable to find a simpler approach that would still reflect experimental results. This was achieved in the third approach developed by taking elements of both the previous models. The idea of modeling the combustion initiation via a threshold parameter was done by tracking the integration of the Arrhenius global reaction rate for propane. As was the case for the temperature threshold case, this was followed by a gaussian type function to model the reaction rate of fuel. This approach also correlated well with experimental combustion timing.

References

- [1] P.A. Caton, A.J. Simon, J.C. Gerdes, and C.F. Edwards. Residual-effected homogeneous charge compression ignition at low compression ratio using exhaust reinduction. *International Journal of Engine Research*, 4(2), 2003.
- [2] M. Christensen, A. Hultqvist, and B. Johansson. Demonstrating the multi-fuel capability of a homogeneous charge compression ignition engine with variable compression ratio. *SAE paper 1999-01-3679*.
- [3] Scott B. Fiveland and Dennis N. Assanis. A quasi-dimensional HCCI model for performance and emissions studies. *Ninth International Conference on Numerical Combustion*, Paper No. MS052.
- [4] N.B. Kaahaaina, A.J. Simon, P.A. Caton, and C.F. Edwards. Use of dynamic valving to achieve residual-affected combustion. *SAE paper 2001-01-0549*.
- [5] S.C. Kong, C.D. Marriot, R.D. Reitz, and M. Christensen. Modeling and experiments of HCCI engine combustion using detailed chemical kinetics with multidimensional CFD. *Combustion Science and Technology*, 27:31–43, 1981.
- [6] D. Law, D. Kemp, J. Allen, G. Kirkpatrick, and T. Copland. Controlled combustion in an IC-engine with a fully variable valve train. *SAE paper 2001-01-0251*.
- [7] Joel Martinez-Frias, Salvador M. Aceves, Daniel Flowers, J. Ray Smith, and Robert Dibble. Hcci engine control by thermal management. *SAE paper 2000-01-2869*.
- [8] Roy Ogink and Valeri Golovitchev. Gasoline HCCI modeling: An engine cycle simulation cosde with a multi-zone combustion model. *SAE paper 2002-01-1745*.
- [9] A.G. Stefanopoulou, J.W. Grizzle, and J.S. Freudenberg. Joint air-fuel ratio and torque regulation using secondary cylinder air flow actuators. *ASME Journal of Dynamic Systems, Measurement, and Control*, 121(4):638–647, 1999.

[10] P. Tunestal, J-O Olsson, and B. Johansson. HCCI operation of a multi-cylinder engine. *First Biennial Meeting of the Scandinavian-Nordic Section of the Combustion Institute*, 2001.

[11] Charles K. Westbrook and Frederick L. Dryer. Simplified reaction mechanisms for the oxidation of hydrocarbon fuels in flames. *Combustion Science and Technology*, 27:31–43, 1981.